2007

# Analysis of Solid-Liquid Phase Change under Pulsed Heating

S. Krishnan

J. Y. Murthy

S V. Garimella
*Purdue University*, sureshg@purdue.edu



Krishnan, S.; Murthy, J. Y.; and Garimella, S V., "Analysis of Solid-Liquid Phase Change under Pulsed Heating" (2007). *CTRC Research Publications.* Paper 265.
http://dx.doi.org/10.1115/1.2430728

# Analysis of Solid–Liquid Phase Change Under Pulsed Heating

**Shankar Krishnan**

**Jayathi Y. Murthy**

**Suresh V. Garimella**
e-mail: sureshg@purdue.edu

Cooling Technologies Research Center,
School of Mechanical Engineering,
Purdue University,
West Lafayette, IN 47907-2088

*Solid/liquid phase change occurring in a rectangular container with and without metal foams subjected to periodic pulsed heating is investigated. Natural convection in the melt is considered. Volume-averaged mass and momentum equations are employed, with the Brinkman–Forchheimer extension to Darcy's law used to model the porous resistance. A local thermal nonequilibrium model, assuming equilibrium melting at the pore scale, is employed for energy transport through the metal foams and the interstitial phase change material (PCM). Separate volume-averaged energy equations for the foam and the PCM are written and are closed using a heat transfer coefficient. The enthalpy method is employed to account for phase change. The governing equations for the PCM without foam are derived from the porous medium equations. The governing equations are solved implicitly using a finite volume method on a fixed grid. The coupled effect of pulse width and natural convection in the melt is found to have a profound effect on the overall melting behavior. The influence of pulse width, Stefan number, and Rayleigh number on the temporal evolution of the melt front location and the melting rate for both the cases with and without metal foams is investigated.*
[DOI: 10.1115/1.2430728]

*Keywords: heat transfer, phase change, porous media, natural convection, nonequilibrium, enhancement*

## Introduction

Solid–liquid phase change [1,2] and cyclic melting and freezing are frequently encountered in latent heat storage systems and have attracted considerable attention for thermal energy storage applications [1]. In these applications, energy is stored in the form of latent heat of fusion during melting, and is recovered during freezing. Detailed reviews of melting and freezing phenomena can be found in Refs. [2–4]. In many electronics applications, periodic thermal transients may occur; examples include electronic power steering controllers, power semiconductors for motor drives and antilock braking controllers.

Though there is extensive literature on solid–liquid phase change [5,6], periodic pulse heating of phase change materials for electronics cooling has received less attention. Periodic melting and freezing in latent heat storage systems for space applications have been studied, and details of the system performance for these applications are available in Refs. [7,8]. However, the frequency of pulses investigated in these applications is usually very low.

A few studies have considered transient phase change for electronics cooling. Lu [9] reported a study of phase-change cooling with emphasis on suppressing the junction temperature rise due to a single high-power pulse. This study also provided design guidelines for high-power electronic packages. Evans et al. [10] analyzed power electronic packages and provided design guidelines relating the materials, geometry, power input, and junction temperature for steady-state conditions and transient pulses. Pal and Joshi [11] investigated numerically the melting of a phase change material (PCM) under transient variations in the power input for passive thermal control of electronic modules.

Commonly used PCMs such as paraffins have very low thermal diffusivity and are not suitable for transient thermal management applications. In order to improve their effective thermal conductivity and enhance heat transfer rates, internal fins or metal foams have been introduced into the PCM [12–14]. Vesligaj and Amon [15] investigated passive thermal control of portable electronics using PCMs with thermal conductivity enhancers under unsteady thermal workloads. Alawadhi and Amon [16] also studied phase change inside enclosures with metal fins to enhance heat transfer for transient applications. Baker et al. [17] performed an analysis of the thermal control performance of a nonmetallic PCM with metallic fins under periodic heating. They reported significant temperature suppression in periodic heat generating systems with little or no weight penalties for space applications. Similarly, Pal and Joshi considered thermal control of heat sources using metal foams [18]. Harris et al. [19] presented an approximate theoretical model to analyze the phase change process in a porous medium. Assuming equilibrium melting at the pore scale, a parametric study based on a semi-heuristic conduction model was formulated. The conditions for the existence of local thermal equilibrium were explored.

The objective of the present work is to investigate the problem of solid–liquid phase change occurring in a rectangular enclosure under pulsed heating from one side. The effect of incorporating metal foams in the enclosure is considered. The difference in response time between systems with and without metal foam has important implications for the thermal management of transient energy pulses [20]. If the time scale of the energy pulse is short compared to the response time of the heat sinking system, local overheating is possible. The presence of a metal foam decreases the response time substantially, and thus PCM systems with metal foams perform significantly better than those without metal foams. The objective of the present study is to investigate the influence of pulse width, Stefan number, and Rayleigh number on the temporal evolution of the melt front location (melting rate) and heat transfer from the active wall with and without metal foams. This work is a follow up to previous studies on metal foams by the authors [13,14], in which a constant heat input was provided to the domain with and without metal foams being present.

## Mathematical Model

A schematic diagram of the problem under investigation is shown in Fig. 1. The square domain of side $H$ encloses the metal foam and PCM. The vertical wall on the right is maintained at a constant temperature $T_C$. The top and bottom walls are adiabatic. The metal foam and the PCM are at equilibrium at temperature $T_C^*$, initially. At time $\tau=0$, a rectangular pulsed temperature condition as shown in Fig. 1 is applied to the vertical wall on the left. The applied temperature alternates between the hot wall temperature, $T_H > T_{\text{melt}}$, and the cold wall temperature, $T_C < T_{\text{melt}}$. The thermophysical properties of the solid metal foam and the PCM are assumed to be constant over the range of temperatures considered. The liquid PCM is assumed to be incompressible, Newtonian, and subject to the Boussinesq approximation. Volume change due to phase change is ignored, as are thermal dispersion effects. Using the dimensionless variables

Contributed by the Heat Transfer Division of ASME for publication in the JOURNAL OF HEAT TRANSFER. Manuscript received February 6, 2006; final manuscript received August 14, 2006. Review conducted by Jose L. Lage. Paper presented at the 2005 ASME International Mechanical Engineering Congress (IMECE2005), Orlando, FL, USA, November 5–11, 2005.

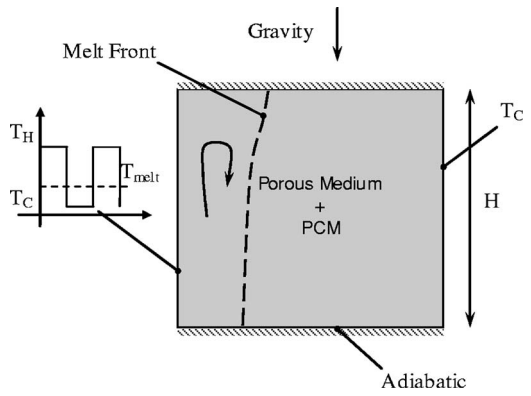


**Fig. 1 Schematic diagram of the problem under investigation**

$$\xi = \frac{x}{H}; \quad \eta = \frac{y}{H}; \quad \tau = \frac{t\alpha_f}{H^2}; \quad U = \frac{uH}{\alpha_f}; \quad P = \frac{pH^2}{\rho_f \nu_f \alpha_f}$$

$$T_s^* = \frac{(T_m - T_c)}{(T_H - T_C)}; \quad T_f^* = \frac{(T_f - T_C)}{(T_H - T_C)}; \quad T^* = \frac{(T - T_C)}{(T_H - T_C)}$$

the dimensionless equations governing the conservation of mass, momentum and energy are

$$\nabla \cdot \mathbf{U} = 0 \tag{1}$$

$$\frac{1}{\mathrm{Pr}}\left(\frac{1}{\varphi}\frac{\partial \mathbf{U}}{\partial \tau} + \frac{1}{\varphi^2}(\mathbf{U}\cdot\nabla)\mathbf{U}\right) = -\nabla \mathbf{P} + \frac{1}{\varphi}\nabla^2 \mathbf{U} - \left(\frac{1}{\mathrm{Da}^2} + \frac{F}{\mathrm{Pr}\cdot\mathrm{Da}}|\mathbf{U}|\right)\mathbf{U} + \mathrm{Ra}\, T_f^* \frac{\boldsymbol{g}}{|\boldsymbol{g}|} \tag{2}$$

$$(1-\varepsilon)\Omega\frac{\partial T_m^*}{\partial \tau} = (1-\varepsilon)\lambda\nabla^2 T_m^* - \mathrm{Nu}_i(T_m^* - T_f^*) \tag{3}$$

$$\varepsilon\frac{\partial T_f^*}{\partial \tau} + (\mathbf{U}\cdot\nabla)T_f^* = \varepsilon\nabla^2 T_f^* - \frac{\varepsilon}{\mathrm{Ste}}\frac{\partial \gamma}{\partial \tau} - \mathrm{Nu}_i(T_f^* - T_m^*) \tag{4}$$

In the above equations, $F$ is the inertial coefficient; $\gamma$ is the fraction of liquid in the PCM ($\gamma = V_l/V_f$); and $\varphi$ is the fraction of liquid PCM in the given volume ($\varphi = \gamma\varepsilon$). The energy equations are closed using a heat exchange term. Details of the mathematical model can be found in Refs. [13,14]. A detailed discussion of the numerical methods employed for solving Eqs. (1)–(4), as well as code validation, and grid- and time-step independence are also available in Refs. [13,14] and are not repeated here. A nonuniform grid of $102 \times 102$ is employed for all the computations.

The inertial coefficient, $F$, for flow through metal foams is 0.068 [21]. The melting point of the PCM is maintained constant at $T_{\mathrm{melt}}^* = 0.3$ for the calculations presented below. For metal foams, a constant porosity of 0.8 is used for all the computations. For organic PCMs ($\mathrm{Pr} > 25$) undergoing phase change in porous enclosures, the velocities encountered are small ($\sim O(10^{-3})$ m/s or less) for $\mathrm{Ra}\,\mathrm{Da}^2 \leq 10^4$. As the system is expected to be largely conduction dominated, it is critical to establish the diffusion limit for the interstitial heat transfer coefficients. The interstitial Nusselt number based on the pore diameter used for all the calculations is 5.9, based on the expression of Morgan [22] for flow over cylinders at the conduction limit. The details of the calculations and the effect of different interstitial Nusselt numbers on the heat transfer characteristics of metal foam-integrated PCM enclosures are available in Ref. [14]. For the periodic heat input studied here, two different pulse widths $\tau_w$ are chosen corresponding to: (i) the time for natural convection to just set in ($\tau_w \sim 9\,\mathrm{Ra}^{-1/2}/\mathrm{Ste}$) [5]; and (ii) the time for the entire PCM to melt completely.

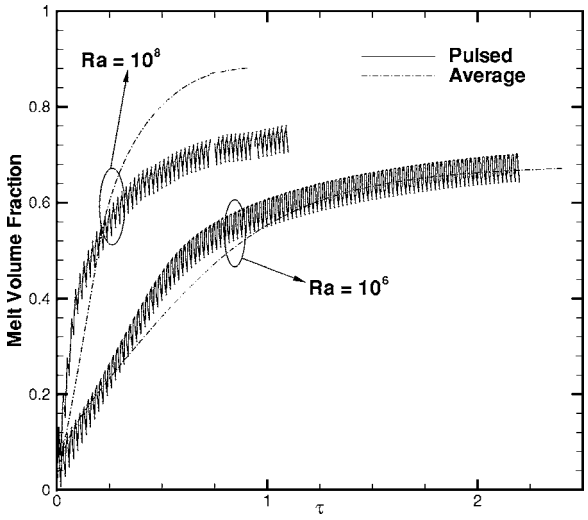


**Fig. 2 Predicted temporal evolution of melt volume fraction for two different Rayleigh numbers ($\mathrm{Ra} = 10^6, 10^8$), Ste=1, Pr =50, and $\tau_w = 0.01$**

## Results and Discussion

Melting of a pure phase change material (without foam) is first considered, followed by an investigation of the effects of the presence of a foam. The Prandtl number of the PCM material is 50, and the nondimensional melting temperature is fixed at 0.3. Further, the solid- and liquid-phase thermophysical properties of the PCM are assumed to be equal and constant. For the pure materials, the nondimensional pulse widths ($\tau_w$) analyzed are 0.01 and 0.22. For a constant left wall temperature ($T_H^*$), the melting process in a rectangular enclosure follows a sequence of four regimes, each characterized by a unique Nusselt number [5,14]: (1) conduction ($\mathrm{Nu} \sim ((\mathrm{Ste}_H \tau)^{-1/2})$); (2) mixed conduction plus convection ($\mathrm{Nu} \sim ((\mathrm{Ste}_H \tau)^{-1/2} + \mathrm{Ra}(\mathrm{Ste}_H \tau)^{3/2})$); (3) convection ($\mathrm{Nu} \sim \mathrm{Ra}^{1/4}$), and (4) shrinking solid regimes. Here, $\mathrm{Ste}_H = C_{pf}(T_H - T_{\mathrm{melt}})/\Delta H$, and is based on the temperature difference ($T_H - T_{\mathrm{melt}}$) and the PCM's specific heat, $C_{pf}$, which is assumed to be the same for both solid and fluid phases. Detailed discussions of the four regimes are given in Refs. [5,14]. It should be noted that the Nusselt number is time dependent in the conduction and conduction-plus-convection regime, but is time invariant during the quasi-steady convection regime. For boundary temperatures oscillating above and below the melting temperature of the PCM, melting occurs during the hot period followed by solidification during the cold period. If the pulse width is shorter than the "steady-state" time required for melting, then the melting process will not evolve through all the four different regimes.

Figure 2 shows the predicted PCM melt volume fraction at two different Rayleigh numbers, for a pulse width of 0.01. The Stefan number in the plots in this work is based on the melting period, i.e., $\mathrm{Ste}_H = C_{pf}(T_H - T_{\mathrm{melt}})/\Delta H$. The phase change process for $\mathrm{Ra} = 10^6$ and $10^8$ reaches a periodic steady-state over a nondimensional time of approximately 2 and 0.5, respectively. The time for convection to set in during the melting process is given by $9\,\mathrm{Ra}^{-0.5}/\mathrm{Ste}$ [5]; this time scale is derived assuming that the initial temperature of the domain is at the melting point.

For cases in which $\tau_w < 9\,\mathrm{Ra}^{-0.5}/\mathrm{Ste}$, i.e., for $\mathrm{Ra} = 10^6$, the process is expected to be conduction dominated. For oscillating boundary conditions with high-frequency pulsing, the boundary layer response in conduction-dominated flow is confined to a thin region adjacent to the surface. The thickness of the region over which the pulse is felt is $\sim(\alpha_{ef}/f)^{1/2}$ in which $f$ is the frequency of the pulses and $\alpha_{ef} = k/(\rho(C_p)_{ef})$ where $(C_p)_{ef} \sim \Delta H/\Delta T$. In non-

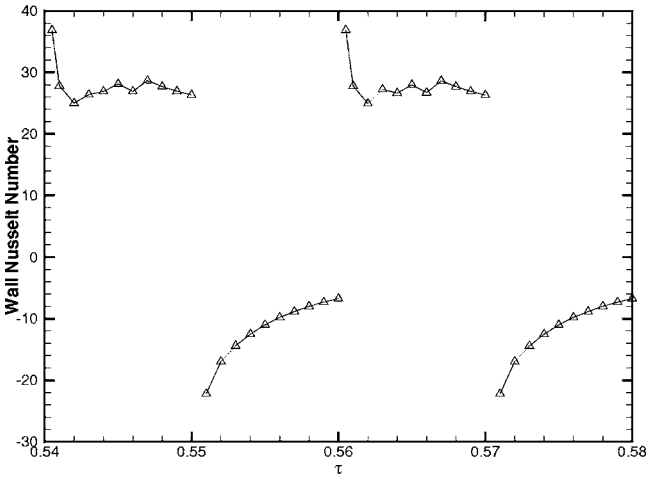


**Fig. 3 Predicted wall Nusselt number for a Ra=$10^8$, Ste=1.0, Pr=50, and $\tau_w$=0.01 at periodic steady state**

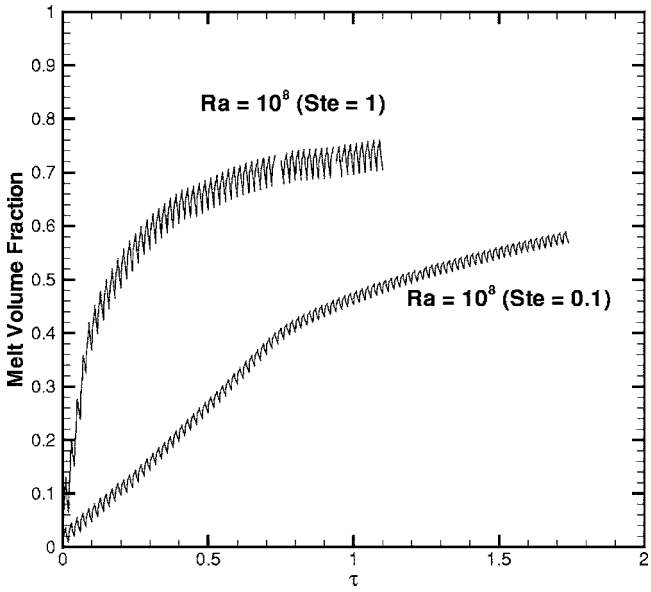


**Fig. 4 Temporal evolution of predicted melt volume fraction for two different Stefan numbers (0.1 and 1.0) and for Ra=$10^8$, Pr=50, and $\tau_w$=0.01**

dimensional terms, this length scale may be written as $(\alpha \mathrm{Ste}/f)^{1/2}/H$, where Ste takes appropriate values during the hot and cold periods. Since both the melting and solidification processes are conduction dominated for Ra=$10^6$, it is expected that an average amount of energy, corresponding approximately to a steady boundary temperature of $(T_H^*+T_C^*)/2$, enters the domain in each cycle. This "averaged" behavior is best illustrated by comparing the low-Ra behavior with the transient response of an enclosure with the left wall raised to $(T_H^*+T_C^*)/2$ at $\tau=0$ and held at this constant temperature. The melt volume fraction for this case is shown in Fig. 2 and is labeled "average." The pulsed case at Ra=$10^6$ follows the "average" case closely.

In contrast, for Ra=$10^8$, the pulse width $\tau_w > 9\ \mathrm{Ra}^{-0.5}/\mathrm{Ste}$ and the phase change process enters a quasi-steady convection regime in which the melt volume fraction scales as $\mathrm{Ra}^{0.25}\mathrm{Ste}\ \tau$. As seen in Fig. 2, the correspondence between the net heat input into the domain in the pulsed case and that for a fixed average boundary temperature ("average" case) is no longer present when there is significant convection. It should be noted that for the average cases, the actual Rayleigh and Stefan numbers take half the values of the equivalent pulsed cases.

Figure 3 shows the predicted wall Nusselt number once a periodic steady state is achieved for Ra=$10^8$, Ste=1.0, and $\tau_w$=0.01. The wall Nusselt number is calculated using the expression

$$\mathrm{Nu} = \frac{hH}{k_f} = (-1)\int_0^1 \left(\frac{\partial T^*}{\partial \xi}\right)_{\xi=0} d\eta \tag{5}$$

The heat extraction period in each pulse is denoted by negative Nusselt numbers. At $\tau=0$, the Nusselt number is theoretically infinite, and this is also true at the instant when the left wall temperature changes from hot to cold (this is represented in the plots as a break in the Nusselt number curves). As the melting process evolves, as discussed before, it follows a sequence of distinct regimes characterized by unique Nusselt numbers. It should be noted that the Nusselt number curves (at a periodic steady state) during the hot periods of the pulsed boundary temperature are very similar to those for a constant boundary temperature as discussed in Ref. [14] for Ra=$10^8$ and Ste=1.0. When the temperature on the left wall changes from $T_H^*$ to $T_C^*$, solid begins to grow from the left wall (at the rate of $\tau^{1/2}$ where $\mathrm{Nu} \propto \tau^{-1/2}$ [3]) until the beginning of the next period, at which time the cycle is repeated.

The effect of Stefan number is brought out in Fig. 4 for Ra=$10^8$. Here again, the pulse width $\tau_w$ is 0.01. If the imposed temperature boundary conditions were constant and not pulsed, the Stefan number would be inversely proportional to the time taken to reach steady state, i.e., $\tau_{ss} \propto \mathrm{Ste}^{-1}$. With an oscillating temperature boundary condition, the change in Stefan number affects the average melt volume fraction for a given cycle (in both the hot and cold periods) and also the total dimensionless time to reach a periodic steady state. It may be recalled that the process is conduction dominated during both the melting and resolidification periods for Ste=0.1. The same is not true for Ste=1.0 in this case, natural convection is established during the melting period. Thus it can be seen that there is a strong dependence of the melt volume fraction on the Stefan number.

Figure 5 shows the effect of pulse width variation from $\tau_w$=0.01 and 0.22, for Ra=$10^8$, and Ste=1.0. For a nondimensional pulse width $\tau_w$=0.22, the phase change process establishes a steady state even before the end of the pulse. This can be clearly seen in Fig. 5. It should be noted that the pulse width affects the total melted material during a given cycle and also the system periodic steady-state time scale.

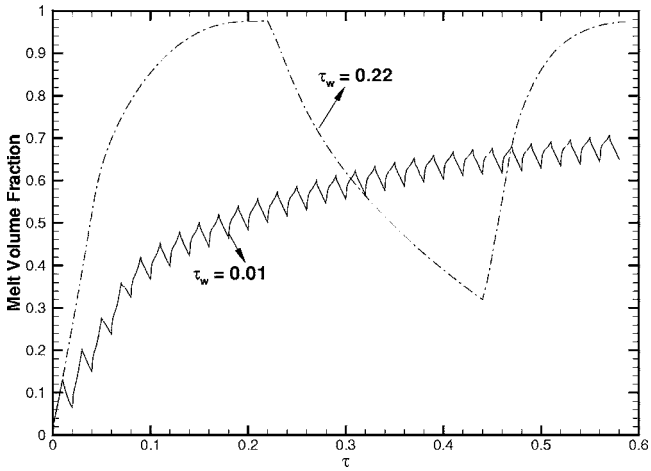


**Fig. 5 Predicted temporal evolution of the melt volume fraction for Ra=$10^8$, Ste=1.0, Pr=50, and two different pulse widths ($\tau_w$=0.01 and 0.22)**

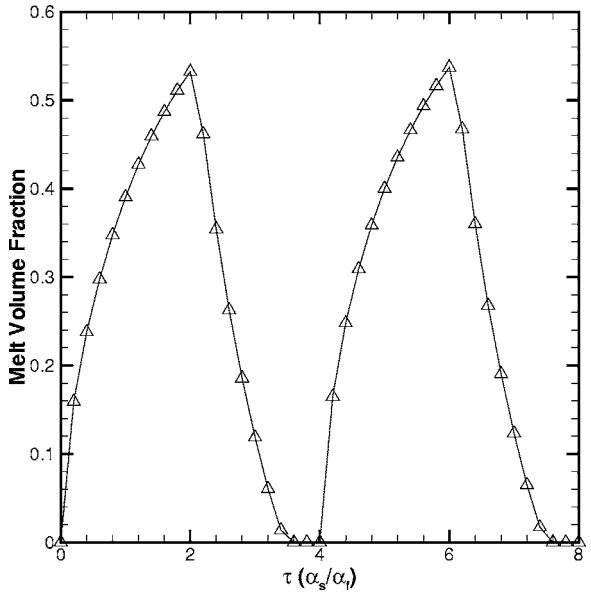


**Fig. 6 Predicted melt volume fraction for Ra=$10^6$, Pr=50, Da=$10^{-2}$, Ste=1.0, and $\tau_w$=0.002**

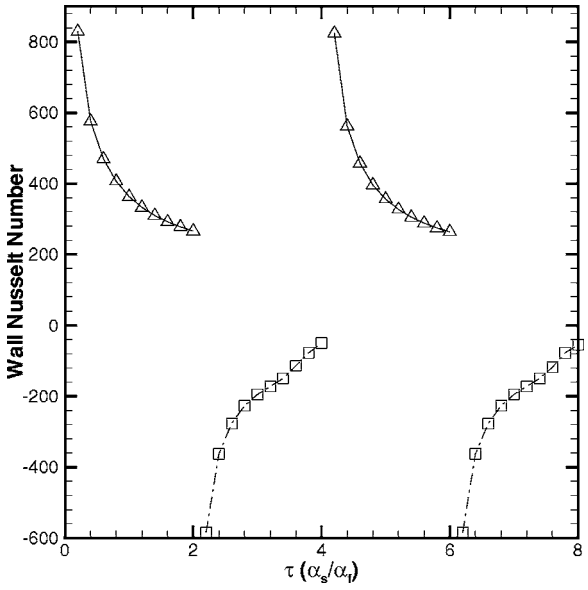


**Fig. 7 Predicted wall Nusselt number for Ra=$10^6$, Pr=50, Da=$10^{-2}$, Ste=1.0, and $\tau_w$=0.002**

**Metal Foams.** Metal foams impregnated with PCMs are considered next. The porosity of the metal foam is held constant at 0.8 with a pore size ($d/H$) of 0.0135. The ratio of the average ligament diameter of the foam to the mean cell size is 0.1875, with the average ligament diameter being 0.36 mm. The ratio of the metal foam-to-PCM thermal conductivity ($\lambda$) is 1000, while the ratio of thermal capacitances ($\Omega$) is unity. The nondimensional melting temperature of the PCM is fixed at 0.3. The metal foam–PCM system steady state is dictated by the time for heat exchange between the metal foam and the PCM, $(1-\varepsilon)\Omega/\mathrm{Nu}_i$ [14]. As long as the heat exchange time is short compared to the response times of the two phases (PCM and metal foam), the two phases develop together in a coupled manner and the time to steady state is determined by the faster phase [14]. Therefore, it is expected that the time to reach steady state for the foam–PCM system is dictated by the metal foam response time ($\sim\Omega/\lambda$) due to the short heat exchange time between the two phases. A detailed discussion of the foam–PCM composite time scales and the effect of interstitial Nusselt number and temperature fields on the heat transfer characteristics for a constant temperature boundary condition can be found in Ref. [14]. The response time for the metal foam–PCM composite is faster by $O(10^{-3})$ than the PCM-only case discussed earlier. After initial computational experiments with constant temperature boundary conditions (not discussed here), it was found that the metal foam–PCM system reached a steady state at a dimensionless time of 0.008. Hence, the pulse widths employed in the following discussions, 0.002 and 0.008, are much shorter than for the PCM-only cases discussed before.

Figure 6 shows the melt volume fraction as a function of $\tau(\alpha_s/\alpha_f)$ for Ra=$10^6$, $\tau_w$=0.002, Ste=1, $\varepsilon$=0.8, Pr=50, Da=$10^{-2}$, and interstitial Nusselt number of 5.9. Since metal foam is the dominating scale, the dimensionless time is renormalized in terms of thermal diffusivity of the foam $\alpha_s$. When $\mathrm{Nu}_i > (1-\varepsilon)\lambda$, the interphase heat exchange time is shorter than the diffusion time for metal foam (which is the fast-response phase) and the system steady state is dictated by the metal foam time scale. In the presence of the foam during the melting period, convective flow in the melt is impeded due to low values of the parameter $\mathrm{Ra\,Da}^2$(=100). Conduction-dominated profiles result, limiting the maximum possible melt volume fraction to $(1-T^*_{\mathrm{melt}})$ [14], i.e., both the temperature profile in the metal foam and the PCM are straight lines and the melt volume fraction is thus the region $T^* > T^*_{\mathrm{melt}}$. As expected for $\tau_w < \Omega/\lambda$, the melt volume fraction is less than $(1-T^*_{\mathrm{melt}})$. During the cold pulse period, the system steady state again is dictated by the metal foam, and the PCM foam cools off before the end of the pulse, i.e., the system reaches a periodic steady state much faster than the no-foam case discussed, by almost $O(10^{-2})$.

Figure 7 shows the Nusselt number at the hot wall for the case considered in Figure 6. The Nusselt number is defined as

$$\mathrm{Nu}_{\mathrm{total}} = \mathrm{Nu}_m + \mathrm{Nu}_f = -(1-\varepsilon)\lambda \int_0^1 \left(\frac{\partial T^*_m}{\partial \xi}\right)_{\xi=0} d\eta - \varepsilon \int_0^1 \left(\frac{\partial T^*_f}{\partial \xi}\right)_{\xi=0} d\eta \tag{6}$$

It should be noted that in Fig. 6, that the $x$ axis is plotted in terms of $\tau(\alpha_s/\alpha_f)$. Initially, the heat transfer from the wall is large, but it drops rapidly as both the metal and PCM heat up. In the presence of foam, heat transfer is conduction dominated, and at steady state, the dimensionless temperature gradient at the wall for both metal foam and PCM is unity. Hence, for a constant temperature boundary condition, the Nusselt number asymptotes (drops) to $\mathrm{Nu}_{\mathrm{total}} \sim \varepsilon + (1-\varepsilon)\lambda$ at steady state. Since $\tau_w < \tau_{\mathrm{ss}}$, $\mathrm{Nu}_{\mathrm{total}}$ is higher than $\varepsilon + (1-\varepsilon)\lambda$. It can be seen from Fig. 7 that $\mathrm{Nu}_{\mathrm{total}} \to 0$ as the cold part of the cycle progresses, since the left and right walls are both subjected to $T^*_C$ during this period. It should be noted that the Nusselt number for the case with foam is higher by an order of magnitude compared to the no-foam case discussed earlier.

The pulses of longer duration, in which the pulse width is chosen such that the phase change process reaches a steady state before the end of the hot period, are considered next. Figure 8 shows the melt volume fraction as a function of $\tau(\alpha_s/\alpha_f)$ for Ra=$10^6$, $\tau_w$=0.008, Ste=1, $\varepsilon$=0.8, Pr=50, Da=$10^{-2}$, and interstitial Nusselt number of 5.9. Since the process is conduction dominated, the system reaches a periodic steady state as discussed for the previous case. The increase in pulse width increases the amount of melted PCM during the hot period. As discussed before, the melt volume fraction asymptotes to $(1-T^*_{\mathrm{melt}})$. During the cold pulse period, the PCM-foam system cools off before the end of the

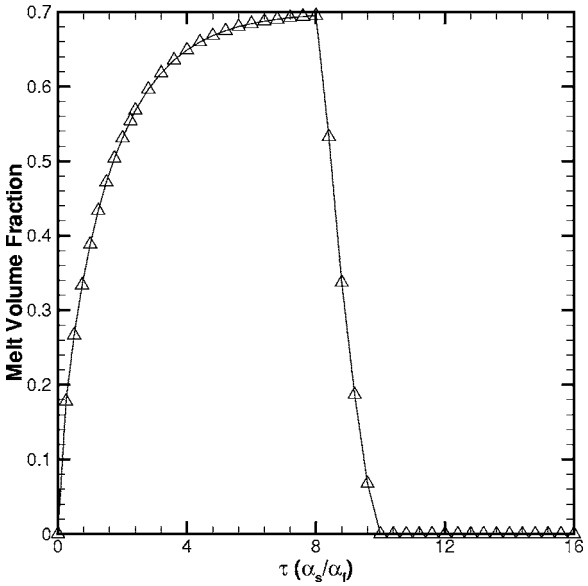


**Fig. 8 Predicted melt volume fraction for Ra=$10^6$, Pr = 50, Da=$10^{-2}$, Ste=1.0, and $\tau_w$=0.008**

pulse.

When the Rayleigh number is increased from $10^6$ to $10^8$ (results not shown), the melt volume fraction at periodic steady state increases from 0.7 to 0.74; however, the overall behavior is similar to that for Ra=$10^6$ as discussed above. Similarly, a decrease in Stefan number from 1.0 to 0.1 with Ra=$10^6$ (results not shown) decreases the rate of melting due to the thermal inertia associated with phase change and the concomitant relative increase in the latent heat of fusion.

## Conclusions

Solid/liquid phase change occurring in a rectangular container with and without metal foams under periodic pulsed heating is investigated. For the case of a pure PCM without a metal foam, the combined effect of pulse width and natural convection in the melt is found to have a profound effect on the overall melting behavior. For a pulse width $\tau_w < \mathrm{Ra}^{-0.25}/\mathrm{Ste}$, the phase change process exhibits an averaged behavior corresponding to steady wall heating at the mean wall temperature. For $\tau_w > \mathrm{Ra}^{-0.25}/\mathrm{Ste}$, natural convection effects becomes important and averaged behavior is not recovered.

For the metal foam–PCM composite case investigated, the heat transfer process is conduction dominated, irrespective of the pulse width value. The response time for the metal foam–PCM composite is faster by $O(10^{-3})$ than the PCM-only case. Since this time scale is relatively short, a periodic steady state is established rapidly in PCM-impregnated metal foams.

## Acknowledgment

Support for this work from industry members of the Cooling Technologies Research Center, an NSF Industry/University Cooperative Research Center (www.ecn.purdue.edu/CTRC), is gratefully acknowledged.

## Nomenclature

$C_p$ = isobaric specific heat, J kg$^{-1}$ K$^{-1}$
Da = Darcy number (K$^{1/2}$/H)
$d$ = mean pore diameter (m)
$f$ = frequency (s$^{-1}$)
$F$ = inertial coefficient
$g$ = gravity vector (ms$^{-2}$)
$H$ = height of the enclosure (m)
$h_v$ = volumetric heat transfer coefficient (W m$^{-3}$ K$^{-1}$)
$K$ = permeability (m$^2$)
$k$ = thermal conductivity (W m$^{-1}$ K$^{-1}$)
$k_e$ = equivalent thermal conductivity (W m$^{-1}$ K$^{-1}$)
$\mathrm{Nu}_i$ = interstitial Nusselt number ($h_v H^2/k_f$)
$\mathrm{Nu}_{i,d}$ = interstitial Nusselt number based on pore diameter
$P$ = pressure (N m$^{-2}$)
Pr = Prandtl number ($\nu_f/\alpha_f$)
Ra = Rayleigh number ($g\beta H^3(T_H-T_C)/(\alpha_f\nu_f)$)
Ste = Stefan number ($(C_p)_f(T_H-T_C)/\Delta H$)
$T$ = temperature (K)
$t$ = time (s)
$U$ = velocity vector (ms$^{-1}$)
$V$ = volume (m$^3$)
$u,v$ = velocity in $x$ and $y$ directions (ms$^{-1}$)
$x,y$ = Cartesian coordinates

### Greek Symbols

$\alpha$ = thermal diffusivity (m$^2$ s$^{-1}$)
$\beta$ = coefficient of thermal expansion (K$^{-1}$)
$\Delta H$ = enthalpy of freezing/melting (J kg$^{-1}$)
$\varepsilon$ = Porosity
$\gamma$ = fraction of liquid melt in the PCM
$\eta$ = dimensionless $y$ coordinate
$\varphi$ = fraction of liquid PCM ($=\varepsilon\gamma$)
$\lambda$ = conductivity ratio of foam and PCM ($k_m/k_f$)
$\mu$ = dynamic viscosity (N s m$^{-2}$)
$\rho$ = density (kg m$^{-3}$)
$\tau$ = dimensionless time
$\nu$ = kinematic viscosity (m$^2$ s$^{-1}$)
$\xi$ = dimensionless $x$ coordinate
$\Omega$ = volumetric heat capacity ratio of foam and PCM $(\rho C_p)_m/(\rho C_p)_f$

### Subscripts

$C$ = cold
$d$ = diameter
ef = effective fluid property
$f$ = PCM
$H$ = hot; height of enclosure
$l$ = liquid
$p$ = pore or particle
$m$ = metal foam
$s$ = solid (PCM)
ss = steady state
$w$ = pulse width

### Superscripts

$*$ = dimensionless quantity

## References

[1] Humphries, W. R., and Griggs, E. L., 1974, *A Design Handbook of Phase Change Thermal Control and Energy Storage Devices*, NASA, Greenbelt, MD.
[2] Yao, L. S., and Prusa, J., 1989, "Melting and Freezing," Adv. Heat Transfer, **19**, pp. 1–95.
[3] Alexiades, V., and Solomon, A. D., 1993, *Mathematical Modeling of Melting and Freezing Processes*, Hemisphere, Washington, D.C.
[4] Viskanta, R., 1991, "Phase Change Heat Transfer in Porous Media," *Proceedings of 3rd International Symposium on Cold Region Heat Transfer*, Fairbanks, AK, June 11–14, pp. 1–24.
[5] Jany, P., and Bejan, A., 1988, "Scaling of Melting with Natural Convection in an Enclosure," Int. J. Heat Mass Transfer, **31**, pp. 1221–1235.
[6] Gau, C., and Viskanta, R., 1986, "Melting and Solidification of a Pure Metal on a Vertical Wall," ASME J. Heat Transfer, **108**, pp. 174–181.
[7] Hasan, M., Majumdar, A. S., and Weber, M. E., 1991, "Cyclic Melting and Freezing," Chem. Eng. Sci., **46**, pp. 1573–1587.

[8] Yimer, B., 1997, "Phase Change Heat Transfer During Cyclic Heating and Cooling with Internal Radiation and Temperature Dependent Properties," *Proceedings of National Heat Transfer Conference*, Baltimore, August 8–12, ASME, New York, HTD-Vol. 342, pp. 141–146.
[9] Lu, T. J., 2000, "Thermal Management of High Power Electronics with Phase Change Cooling," Int. J. Heat Mass Transfer, **43**, pp. 2245–2256.
[10] Evans, A. G., He, M. Y., Hutchinson, J. W., and Shaw, M., 2001, "Temperature Distribution in Advanced Power Electronics Systems and the Effect of Phase Change Materials on Temperature Suppression During Power Pulses," ASME J. Electron. Packag., **123**, pp. 211–217.
[11] Pal, D., and Joshi, Y., 1997, "Application of Phase Change Materials to Thermal Control of Electronic Modules: A Computational Study," ASME J. Electron. Packag., **119**, pp. 40–50.
[12] Shatikian, V., Dubovsky, V., Ziskind, G., and Letan, R., 2003, "Simulation of PCM Melting and Solidification in a Partitioned Storage Unit," ASME Paper No. HT2003-47167.
[13] Krishnan, S., Murthy, J. Y., and Garimella, S. V., 2004, "A Two-Temperature Model for Analysis of Passive Thermal Control Systems," ASME J. Heat Transfer, **126**, pp. 628–637.
[14] Krishnan, S., Murthy, J. Y., and Garimella, S. V., 2005, "A Two-Temperature Model for Solid-Liquid Phase Change in Metal Foams," ASME J. Heat Transfer, **127**, pp. 995–1004.
[15] Vesligaj, M. J., and Amon, C. H., 1999, "Transient Thermal Management of Temperature Fluctuations during Time Varying Workloads on Portable Electronics," IEEE Trans. Compon. Packag. Technol., **22**, pp. 541–550.
[16] Alawadhi, E. M., and Amon, C. H., 2000, "Performance Analysis of an Enhanced PCM Thermal Control Unit," *Proceedings of ITherm 2000*, Las Vegas, NV, May 24–26, pp. 283–289.
[17] Baker, K. W., Jang, J. H., and Yu, J. S., 1995, "Thermal Control of Phase Change Package with Periodic Pulse Heating—A Case Study," *Proceedings of ASME/JSME Thermal Engineering Conference*, Maui, HI, March 19–24, ASME, New York, 4, pp. 463–469.
[18] Pal, D., and Joshi, Y., 1999, "Thermal Control of Horizontal Mounted Heat Sources using Phase Change Materials," Adv. Electron. Packag., **26**, pp. 1625-1630.
[19] Harris, K. T., Haji-Sheikh, A., and Agwu Nnanna, A. G., 2001, "Phase-Change Phenomena in Porous Media—A Non-Local Thermal Equilibrium Model," Int. J. Heat Mass Transfer, **44**, pp. 1619–1625.
[20] Krishnan, S., and Garimella, S. V., 2004, "Analysis of a Phase Change Energy Storage System for Pulsed Power Dissipation," IEEE Trans. Compon. Packag. Technol., **27**(1), pp. 191–199.
[21] Hwang, J. J., Hwang, G. J., Yeh, R. H., and Chao, C. H., 2002, "Measurement of Interstitial Convective Heat Transfer Coefficient and Frictional Drag for Flow Across Metal Foams," ASME J. Heat Transfer, **124**, pp. 120–129.
[22] Morgan, V. T., 1975, "The Overall Convective Heat Transfer from Smooth Circular Cylinders," Adv. Heat Transfer, **11**, pp. 199–264.